Research on Engineering Structures & Materials
journal homepage: http://www.jresm.org
Research Group

Research Article

Adhesion strength evaluation for plasma-sprayed coatings based on intensity of singular stress

Nikolay Dolgov[1,2,a], Maris Hauka*[3,b], Leonids Vinogradovs[3,c]

[1]*G.S.Pisarenko Institute for Problems of Strength, Nat. Ac. Sci. of Ukraine, 2 Timiryazevska Str, Kyiv, Ukraine*
[2]*National Transport University, 1 Omelianovycha-Pavlenka Str, Kyiv, Ukraine*
[3]*Department of Aeronautics, Riga Technical University, Riga, Latvia*

Article Info

Article history:
Received 13 Nov 2021
Revised 9 May 2022
Accepted 6 June 2022

Keywords:

Finite Element Method;
Plasma-sprayed coatings;
Tensile testing;
Coated specimens;
Co-Cr alloy

Abstract

This paper presents a new test method, including coated specimen, shear testing procedure, and algorithm for evaluation of critical intensity of singular stress for coating, for more accurate and complete characterization of adhesion strength. A procedure for determining the critical intensity of singular stress for coating is presented in this paper. In this paper, the coated specimen has been analysed in terms of the intensity of singular stress field. The adhesion strength of plasma-sprayed coatings was estimated in terms of the intensity of singular stresses in the vicinity of the free edge of the coating. The finite element analysis for normal and tensile stress distributions of the coated specimens are obtained by using different mesh sizes (fine, medium, and coarse size). Tensile testing of flat metal samples with plasma-sprayed coatings of Co-Cr alloy of various thicknesses (90, 100, 160 μm) was performed. The results show that the adhesion strength of the tested coatings can be represented by a critical stress of 1.34, 0.94, 0.88 MPa $m^{0.43}$ for thicknesses of 90, 100, 160 μm, respectively.

1. Introduction

Experimental studies of specimens with coatings indicate, that the delamination of the coating from the substrate initiates from the free edge of the coating even in absence of an initial crack in the interface [1-4].

The coating delamination of the item initiates from the free edge due to the singularity of stresses. The existing studies of the stress state in deformed coating are taking into account only the concentration of shear stresses in the nearby area of the free edge of the coating [5-7]. So, it is necessary to finally study the stress fields singularity dependency on the coated specimen geometric characteristics, as well as the substrate and coating elasticity characteristics.

The study of the singularity of stress fields was initiated in [8], in which the singularity of stresses in plates of various configurations, from homogeneous as well as composite materials was determined. The distribution of stress in a body formed by dissimilar isotropic elastic materials was considered in the work [9]. The distribution of stress in systems of dissimilar materials was also investigated in the work [10]. The problem for an anisotropic material consisting of a system of anisotropic layers separated by isotropic layers was solved in the work [11]. The problem of determining the singularity of stress fields for wedges made of two different materials was considered in numerous works [12-16].

*Corresponding author: maris.hauka@rtu.lv
[a] orcid.org/0000-0002-3962-7551; [b] orcid.org/0000-0003-2134-7647; [c] 0000-0003-2257-8607;
DOI: http://dx.doi.org/10.17515/resm2022.365ma1113

Research of this field is well covered in reviews [17, 18].

There are various approaches to assessing the stress state in layered materials, both analytical methods [19-23], and numerical methods [23, 24].

The investigation of the stress fields singularity in case of thermal barrier coatings deduced that, if the angle of the free edge is decreases to an angle of 60 degree, the coating durability increases [25, 26].

The goal of this paper is to investigate the singular stress fields that cause the coating delamination.

2. The Evaluation of Stress Fields Intensity in A Coated Sample

The field of stress is determinate as [27, 28]:

$$\begin{aligned}
\sigma_r^c &= \frac{K}{r^{1-\lambda}} f_r^c(\lambda,\theta);\\
\sigma_r^s &= \frac{K}{r^{1-\lambda}} f_r^s(\lambda,\theta);\\
\sigma_\theta^c &= \frac{K}{r^{1-\lambda}} f_\theta^c(\lambda,\theta);\\
\sigma_\theta^s &= \frac{K}{r^{1-\lambda}} f_\theta^s(\lambda,\theta);\\
\tau_{r\theta}^c &= \frac{K}{r^{1-\lambda}} f_{r\theta}^c(\lambda,\theta);\\
\tau_{r\theta}^s &= \frac{K}{r^{1-\lambda}} f_{r\theta}^s(\lambda,\theta),
\end{aligned} \tag{1}$$

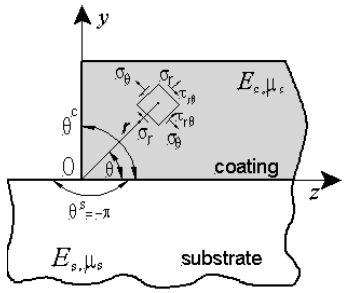

Fig. 1 The detail of "coating"-"substrate" system [28]

The equations for the normal σ_θ^c and shear $\tau_{r\theta}^c$ stresses in the coating from (1) can be written as:

$$\sigma_\theta^c = K_1 r^{\lambda-1} \quad ; \tag{2}$$

$$\tau_{r\theta}^c = K_2 r^{\lambda-1} \quad ;$$

Where,

$$K_1 = Kf_\theta^c(\lambda,\theta);$$

$$K_2 = Kf_{r\theta}^c(\lambda,\theta);$$

Transform the equations (2) to look as:

$$\lg\tau_{r\theta}^c = \lg K_2 + (\lambda - 1)\lg r \quad (3)$$

$$\lg\sigma_\theta^c = \lg K_1 + (\lambda - 1)\lg r$$

From equations (3) it can be determined that there is a linear relationship between stresses and distance *r* if plotting graphs in logarithmic coordinates. If $\lg\sigma_\theta^c$ is shown related to $\lg r$, the graph-line has a slope λ – 1, the graph will intersects the ordinate axis at a point with a y-coordinate $\lg K_1$ Therefore, knowing the value, $\lg\sigma_\theta^c$ at $\lg r = 0$, it is possible to determine the value of $K_1 = 10^{\lg\sigma_\theta^c}$.

3. Methods and Materials

The Co- Cr coating [29, 30] with thickness of 90, 100 and 160 μm has been plasma sprayed on stainless steel substrate (1Kh18N9 stainless steel, containing 0.9% C, 16.7% Cr, 7.8% Ni, 0.37% Si, and 1.47% Mn) thickness 1.5 mm (Fig. 2). The coating was sprayed only partially on steel substrate so as to leave out free edge of the coating (Fig.1). The elastic characteristics of the substrate and the coating were determined under static tension of coated specimen following methodology described in [30].

Fig. 2 Specimen with the plasma sprayed coating (Co- Cr alloy coating; Left view) before the tensile test.

The thickness of the coating is comparatively thick so it is measure using a micrometre. Delamination moment can be fixed through visual observation, as acoustic emission techniques have shown that the moment of coating delamination visually gives an error within 2% boundaries (Not explained further in this study as it is not the object of the research).

The thickness of coating was chosen based on both its intended functionality- to increase wear and corrosion resistance and economic considerations- to not have wasted material. It was proven that coating thickness of 90 μm would start providing some functionality, while thicker coating, while increasing functionality, would increase expenditure in larger scale (Not explained further in this study as it is not the object of the research).

4. Results and Discussion

It should be noted, that the use of the K_{cr} value as a criterion is also possible for coatings in which the angle of the free edge is not equal to 90°. Such coatings are widely used and the deposition of coatings with a free edge angle $\theta_c < 90°$ is recommended by the technological process of plasma coating spraying [31]. The results show that the intensity of singular stresses for the tested metal coatings is dependent weakly on the thickness of the coating. It can be seen, that the analytical method for determining the singularity factor λ is more accurate than the method based on the approximation of stresses obtained using finite element modelling. The critical intensity of singular stress K_{cr}, measured using the proposed technique, can be used as a criterion to evaluate adhesion strength for coatings.

To determine the critical singular stresses that would cause the failure of the coating, the specimen was subjected to tensile load.

The delamination of the coating (sample with coating thickness 90 μm) occurs under stress that corresponds to the moment when the load on the uncoated substrate reach σ_{sub} = 752 MPa.

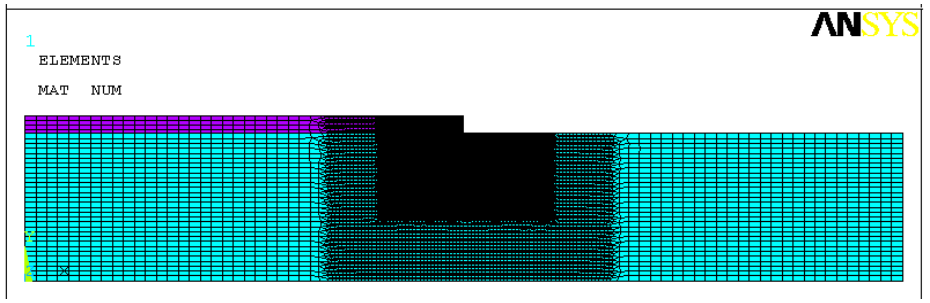

Fig. 3 Coated specimen's finite elements model. Minimal size of mesh 0.2 μm.

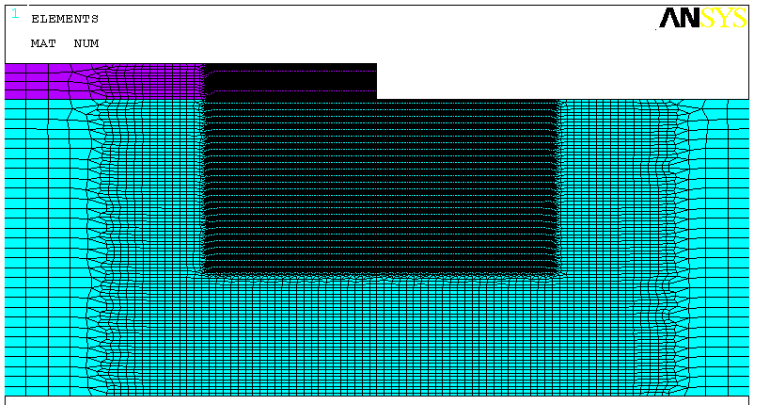

Fig. 4 Part of the finite element mesh model near the free edge of coating and the stress singularity area

The critical stress intensity factor K_{cr} was determined by Finite Element Method (FEM). Specimen's finite element mesh is shown on (Fig.3). The mesh was constructed using half of the specimen. Numerical calculus for elastic solid was made using ANSYS.

The finite element mesh in the area of the singularity was made finer. A fragment of the finite element mesh in the area of stress singularity is shown in (Fig.4); the tensile load was applied to the end face of sample. The minimal size of mesh in the area of stress singularity is 0.2 μm (Fig. 4). The elasticity characteristics of both the coating, and the substrate, were calculated after the tension test as listed in [31], see Table 1.

Table 1. Elasticity characteristics of the coating and its substrate.

	Material	Elastic modulus E, GPa	Poisson Ratio, μ
Substrate	1X18H9	199	0.28
Coating	Co- Cr alloy	70	0.3

The distribution of normal and shear stresses in the area of adhesive contact between the substrate and the coating at a distance r (0.07 ... 100 μm) from the free edge of the coating at = 752 MPa are shown in (Fig.5) (logarithmic coordinates). The distribution of stresses in the sample during the delamination of the coating can be seen in (Fig.6) to (Fig.8).

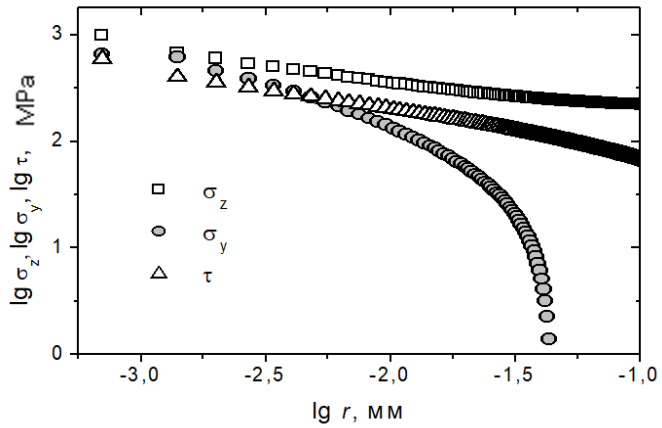

Fig. 5 The distribution of normal and shear stresses in the area of adhesive contact between the substrate and the coating at a distance r (0.07 ... 100 μm) from the free edge of the coating at σ_{sub} = 752 MPa

Deviations from linearity seen in Fig.5 are related to the method used to describe fracture mechanics and estimating the singularity of stresses in the vicinity of a singular point, in particular it is caused by the logarithmic scale.

(Fig.5) shows that the normal tensile stresses σ_z and shear stresses τ vary approximately linearly in the area corresponding to r = 0.7 μm ($\lg r$ = –3.15) to $r \approx$ 14.4 μm ($\lg r \approx$ –1.84). This character of the distribution shows that the stress can be described by the formula given in (2). At r > 14.4 mm the character of these expressions ceases to be linear till eventually the singularity disappears. Normal stresses of the σ_y are linear in a much narrower range of r (0.7 μm < r < 4.8 μm).

The stress σ_y near the free edge of the coating exceeds the shear stresses τ (Fig.5), meaning, in the area of the coating; the free edge delamination occurs due to the predominant action of normal shear stresses σ_y. Consequently, the investigation of how stress singularity affects the coating adhesion failure must be carried out as for normal delamination stresses σ_y.

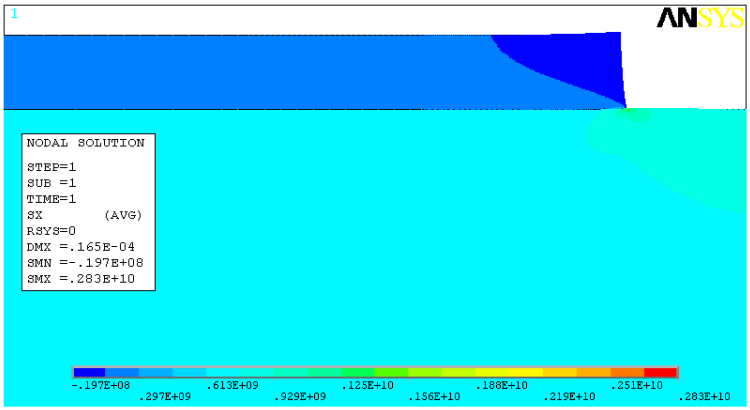

Fig. 6 The distribution of normal stresses σ_z under coating of the specimen during delamination near free edge (σ_{sub} = 752 MPa).

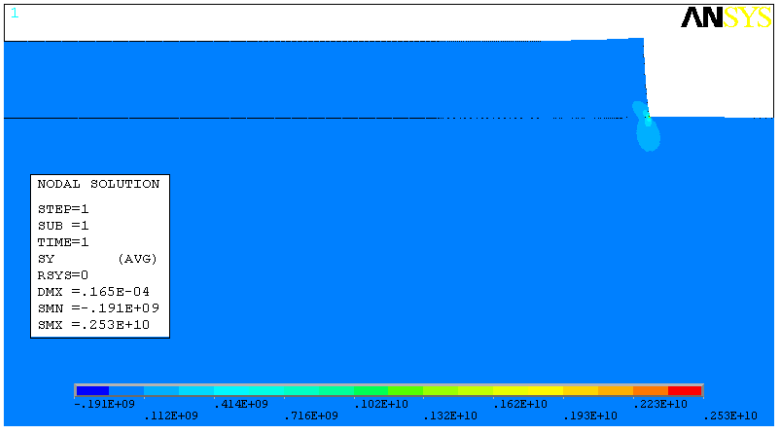

Fig. 7 Normal stresses σ_y distribution under specimen coating delamination near free edge (σ_{sub} = 752 MPa)

As a result of the singularity of the stress near coating free edge [28], the value of the stress might be dependent on how fine the finite element mesh is. To make sure that, the accuracy of K_{cr} does not depends on minimal size of finite element mesh (FEMesh), the simulation was made for three different FEMeshes: sizes; fine 0,2 μm (Fig.8); medium 0.7 μm (Fig. 9); and coarse 6.2 μm (Fig. 10). These simulations allowed to evaluate the area of stress singularity under load σ_{sub} that causes the metal coating delamination. In (Fig.11) normal delamination stresses distribution is shown in three graphs of FEMeshes. Though in the area of the free edge of the coating the stress value depends on FEMeshes size, the curve slope λ–1, does not depend on FEMesh in graph's

linear part $\lg\sigma_y$ compared to $\lg r$. The stresses change is linear in a wide range of *r*, regardless if fine, middle and coarse FEMeshes. The angle of curve slope for expression (3) can be found analytically [28] or by curve-fitting the linear graph part $\lg\sigma_y$ to $\lg r$. Usually such approximation is made using The Least Square Method (LSM). The analytical approach is more accurate than LSM and also allows to determinate two factors of singularity order (the roots λ_1 and λ_2 for characteristic equation).

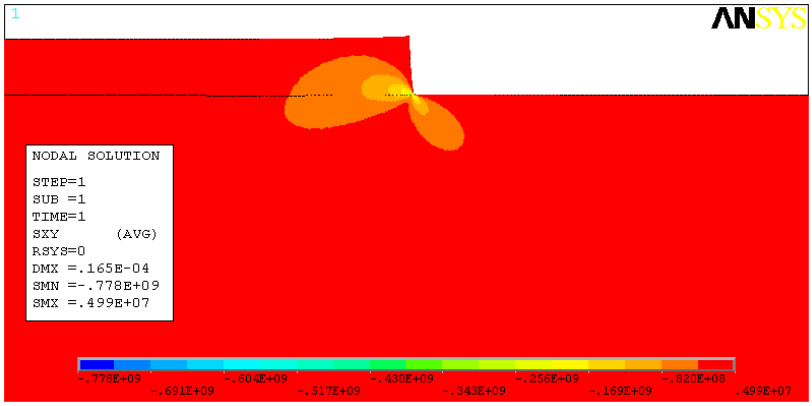

Fig. 8 The shear stresses τ area in a specimen during the coating delamination near its free edge (σ_{sub} = 752 MPa)

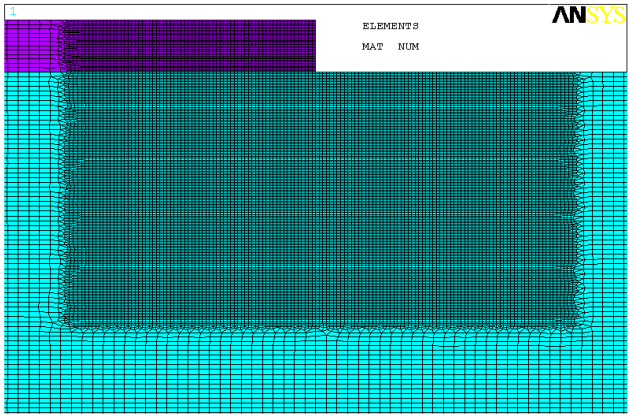

Fig. 9 The FEM of coated specimen (minimal mesh size is 0.7 μm)

When comparing the singularity order calculated by the analytical method with the value obtained by linear approximation by the LSM, it can be concluded that the approximation has errors corresponding to the size of the FEMesh.

The σ_y values obtained by the FEM can be compared with the stresses in accordance with equations (1). The error associated with numerical calculations can be reduced by creating a finer mesh of finite elements.

Plasma-sprayed coatings with a thickness of 100 μm and 160 μm delaminates under loads cause corresponding to stresses of 625 and 340 MPa in the substrate material's uncoated area. A specimen with a coating with a thickness of 160 μm after tensile tests

is shown in (Fig. 12). The indicators of the critical stress intensity K_{cr}, as well as the order of the stress singularity, calculated analytically and found using the approximation method, are given in Table. 2. The stress distribution σ_y near the free edge of the coating during delamination of coatings of various thicknesses is shown in (Fig.13).

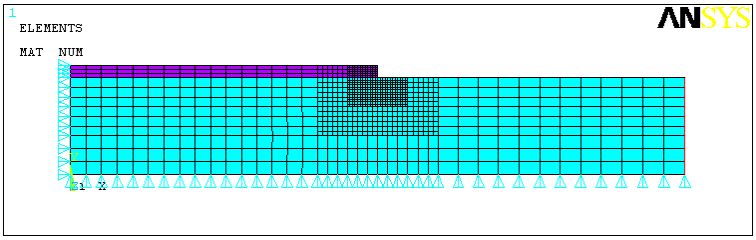

Fig. 10 The FEM of coated specimen (minimal mesh size is 6.2 μm)

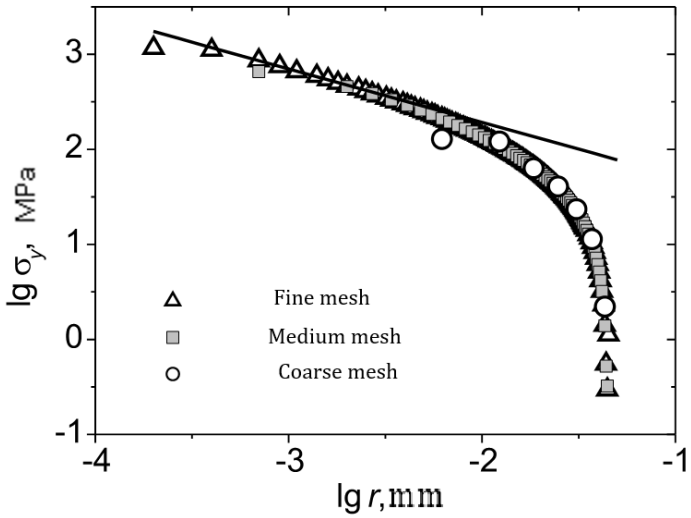

Fig. 11 Impact of FEMeshes size on stress distribution σ_y

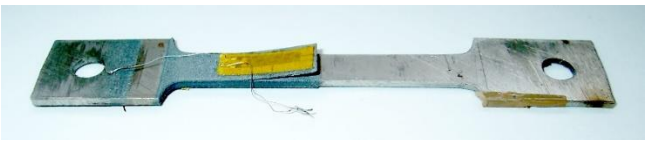

Fig. 12 Plasma-coated (Co-Cr alloy, thickness 160 μm) Sample after tensile load test

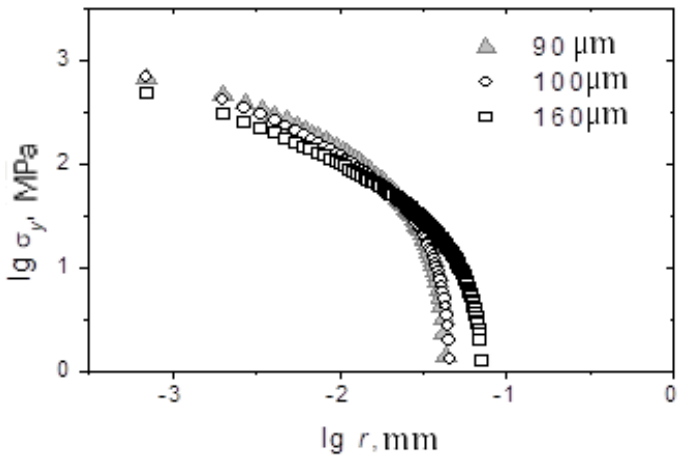

Fig. 13 Stress σ_y distribution during delamination of plasma-sprayed coating of various thicknesses.

Table 2. The Results of Adhesion Properties of plasma-sprayed Coating (Co-Cr alloy) Investigation

Coating thickness h, μm	Factors of stress singularity		Ratio $\frac{\lambda}{\lambda_{num}}$	Critical stress intensity K_{cr}	Physical dimension K_{cr} [MPa·m$^{1-\lambda}$]
	The analytical method [25]	The LSM λ_{num}			
90	0.5687	0.5517	1.031	1.34	MPa·m^{0,43}
100		0.5033	1.130	0.94	
160		0.5429	1.048	0.88	

5. Conclusion

Analysis of the test results shows that the value of K_{cr} for the tested metal coatings is weakly dependent on the thickness of the coating. Thus, the K_{cr} value can be used as a criterion for adhesive destruction of coatings. In addition, it should be noted, that the use of the K_{cr} value as a criterion is also possible for coatings in which the angle of the free edge is not equal to 90°. Such coatings are widely used and the deposition of coatings with a free edge angle $\theta^c < 90°$ is recommended by the technological process of plasma coating spraying. The results show that the intensity of singular stresses for the tested metal coatings is weakly dependent on the thickness of the coating. It can be seen, that the analytical method for determining the singularity factor is more accurate than the method based on the approximation of stresses obtained using finite element modelling. The critical intensity of singular stress, measured using the proposed technique, can be used as a criterion to evaluate adhesion strength for coatings.

Acknowledgement

PostDoc Latvia
NATIONAL DEVELOPMENT PLAN 2020
EUROPEAN UNION
European Regional Development Fund
INVESTING IN YOUR FUTURE

This work has been supported by the European Regional Development Fund within the Activity 1.1.1.2 "Post-doctoral Research Aid" of the Specific Aid Objective 1.1.1 "To increase the research and innovative capacity of scientific institutions of Latvia and the ability to attract external financing, investing in human resources and infrastructure" of the Operational Programme "Growth and Employment" (No. 1.1.1.2/VIAA/2/18/326)

Nomenclature

E - elastic modulus (index c refers to coating, index s refers to substrate);

K- stress intensity factor,

K_{cr} - critical stress intensity factor;

K_1, K_2 – mode 1 and mode 2 stress intensity factors;

f_r^c, f_r^s, f_θ^c, f_θ^s, $f_{r\theta}^c$, $f_{r\theta}^s$ - correcting factor for stresses (index c refers to coating, index s refers to substrate);

r, θ - local polar coordinates;

λ - order of stress singularity.

μ - Poisson Ratio (index c refers to coating, index s refers to substrate);

Q_{sub}- the remote stress applying to the substrate in the z direction;

Q_r, Q_θ, $Q_{r\theta}$ - stress components (index c refers to coating, index s refers to substrate)

σ_y - peeling stress;

σ_z - normal tensile stress;

τ - interfacial shear stress;

FEM - Finite Element Method;

FEMesh - finite element mesh;

LSM - Least Square Method

References

[1] Lyashenko BA, Veremchuk VS, Dolgov NA, Ivanov VM. Strength and deformation properties of compositions with plasma-sprayed coatings. Strength of Materials.1996; 28;452-454. https://doi.org/10.1007/BF02209316

[2]. Shinde SV, Sampath S.. Interplay between cracking and delamination in incrementally deposited plasma sprayed coatings. Acta Materialia, 2021:215; 117074. https://doi.org/10.1016/j.actamat.2021.117074

[3]. Hafez M, Akila S, Khder M, Khalil A. Reducing Cracks and Delamination in Plasma-Sprayed Coatings of Calcia and Magnesia Stabilized-Zirconia. Microscopy and Microanalysis. 2021: 27(S1); 2360-2362. https://doi.org/10.1017/S1431927621008497

[4]. Xiao YQ, Yang L, Zhu W, Zhou YC, Pi ZP, Wei YG. Delamination mechanism of thermal barrier coatings induced by thermal cycling and growth stresses. Engineering Failure Analysis 2021;121:105202. https://doi.org/10.1016/j.engfailanal.2020.105202

[5] Jiang T, Huang R, Zhu Y. Interfacial Sliding and Buckling of Monolayer Graphene on a Stretchable Substrate. Adv Funct Mater 2013;24:396–402. https://doi.org/10.1002/adfm.201301999

[6] Wu K, Wang YQ, Yuan HZ, Zhang JY, Liu G, Sun J. Interfacial stress transfer mechanism of Cu-Zr amorphous films on polyimide substrates: Effect of deformation-induced devitrification. Journal of Alloys and Compounds 2019;783:841–7. https://doi.org/10.1016/j.jallcom.2019.01.016
[7] Panin AV, Shugurov AR, Kazachenok MS, Sergeev VP. Effect of the nanostructuring of a Cu substrate on the fracture of heat-resistant Si-Al-N coatings during uniaxial tension. Tech Phys 2012;57:779–86. https://doi.org/10.1134/s1063784212060205
[8] Williams ML. Stress Singularities Resulting From Various Boundary Conditions in Angular Corners of Plates in Extension. Journal of Applied Mechanics 1952;19:526–8. https://doi.org/10.1115/1.4010553
[9] Bogy DB. Edge-Bonded Dissimilar Orthogonal Elastic Wedges Under Normal and Shear Loading. Journal of Applied Mechanics 1968;35:460–6. https://doi.org/10.1115/1.3601236
[10] Hess MS. The End Problem for a Laminated Elastic Strip — II. Differential Expansion Stresses. Journal of Composite Materials 1969;3:630–41. https://doi.org/10.1177/002199836900300404
[11] Puppo AH, Evensen HA. Interlaminar Shear in Laminated Composites Under Generalized Plane Stress. Journal of Composite Materials 1970;4:204–20. https://doi.org/10.1177/002199837000400206
[12] Chue C-H, Liu C-I. A general solution on stress singularities in an anisotropic wedge. International Journal of Solids and Structures 2001;38:6889–906. https://doi.org/10.1016/s0020-7683(01)00015-4
[13] Luo Y, Subbarayan G. A study of multiple singularities in multi-material wedges and their use in analysis of microelectronic interconnect structures. Engineering Fracture Mechanics 2007;74:416–30. https://doi.org/10.1016/j.engfracmech.2006.04.032
[14] Tan M.A. Analysis of bimaterial wedges using a new singular finite element/ M.A.Tan, S.A.Meguid // International Journal of Fracture. 1997; 88(4):373-391. https://doi.org/10.1023/A:1007427506134
[15] Bogy DB, Wang KC. Stress singularities at interface corners in bonded dissimilar isotropic elastic materials. International Journal of Solids and Structures 1971;7:993–1005. https://doi.org/10.1016/0020-7683(71)90077-1
[16] Dempsey JP, Sinclair GB. On the stress singularities in the plane elasticity of the composite wedge. J Elasticity 1979;9:373–91. https://doi.org/10.1007/bf00044615
[17] Sinclair G. Stress singularities in classical elasticity–I: Removal, interpretation, and analysis. Applied Mechanics Reviews 2004;57:251–98. https://doi.org/10.1115/1.1762503
[18] Sinclair G. Stress singularities in classical elasticity—II: Asymptotic identification. Applied Mechanics Reviews 2004;57:385–439. https://doi.org/10.1115/1.1767846
[19] Agrawal DC, Raj R. Measurement of the ultimate shear strength of a metal-ceramic interface. Acta Metallurgica 1989;37:1265–70. https://doi.org/10.1016/0001-6160(89)90120-x
[20] Dolgov NA, Lyashenko BA, Rushchitskii YaYa, Veremchuk VS, Terletskii VA, Kovalenko AP. Effects of elasticity differences between substrate and coating on the state of stress and strain in a composite. Part 2. Coating tensile stress distribution. Strength Mater 1996;28:373–5. https://doi.org/10.1007/bf02330856
[21] Rizov V. Analysis of cylindrical delamination cracks in multilayered functionally graded non-linear elastic circular shafts under combined loads. Frattura Ed Integrità Strutturale 2018;12:158–77. https://doi.org/10.3221/igf-esis.46.16

[22] Bulbuk O, Velychkovych A, Mazurenko V, Ropyak L, Pryhorovska T. Analytical estimation of tooth strength, restored by direct or indirect restorations. 105267/jEsm 2019:193–204. https://doi.org/10.5267/j.esm.2019.5.004
[23] Li L-A, Li R-J, Wang S-B, Wang Z-Y, Li T, Li C-W. Stress analysis of film-on-substrate structure under tensile loads. Mechanics of Materials 2018;120:1–14. https://doi.org/10.1016/j.mechmat.2018.02.003
[24] Leguillon D, Li J, Martin E. Multi-cracking in brittle thin layers and coatings using a FFM model. European Journal of Mechanics - A/Solids 2017;63:14–21. https://doi.org/10.1016/j.euromechsol.2016.12.003
[25] Brodin H, Li XH, Sjoestroem S. Influence on Thermal Barrier Coating Delamination Behaviour of Edge Geometry. Fracture of Nano and Engineering Materials and Structures n.d.:273–4. https://doi.org/10.1007/1-4020-4972-2_134
[26] Sjöström S, Brodin H. Influence of TBC end geometry on the TMF life of an APS TBC. Procedia Engineering 2010;2:1363–71. https://doi.org/10.1016/j.proeng.2010.03.148
[27] Bogy DB. Two Edge-Bonded Elastic Wedges of Different Materials and Wedge Angles Under Surface Tractions. Journal of Applied Mechanics 1971;38:377–86. https://doi.org/10.1115/1.3408786
[28] Dolgov NA, Soroka EB. Stress singularity in a substrate-coating system. Strength Mater 2004;36:636–42. https://doi.org/10.1007/s11223-005-0010-5
[29] Besov AV, Maslyuk VA, Stepanchuk AN, Napara-Volgina SG, Orlova LN. Cobalt-Chromium Powder Alloys and Retention Coatings Made from Them for Orthopaedic Stomatology. Powder Metall Met Ceram 2005;44:207–10. https://doi.org/10.1007/s11106-005-0082-6
[30] Dolgov NA, Lyashenko BA, Veremchuk VS, Dmitriev YuV. Determining elasticity characteristics for protective coatings. Strength Mater 1995;27:392–4. https://doi.org/10.1007/bf02209364
[31] Handbook of thermal spray technology. (2004) Edited by J.R. Davis. Materials Park, OH: ASM International.